Graphene-organic two-dimensional charge transfer complexes: inter-molecular electronic transitions and broadband near infrared photoresponse

Menghua Cui[†,‡,§], Yuzheng Guo[‖,*], Yiming Zhu[†], Haining Liu[†], Wen Wen[†,§], Juanxia Wu[†], Linxiu Cheng[†], Qingdao Zeng[†] and Liming Xie[†,§,*]

[†]CAS Key Laboratory of Standardization and Measurement for Nanotechnology, CAS Center for Excellence in Nanoscience, National Center for Nanoscience and Technology, Beijing 100190, P. R. China

[‡]Academy for Advanced Interdisciplinary Studies, Peking University, Beijing 100871, P. R. China

[§]University of Chinese Academy of Sciences, Beijing 100049, P. R. China

[‖]College of Engineering, Swansea University, Swansea, SA1 8EN, United Kingdom

Supporting Information Placeholder

ABSTRACT: Charge transfer (CT) complex with unique inter-molecule electronic transitions has attracted broad interest and holds great potentials in optoelectronic applications. Here, we report a new family of two-dimensional graphene-organic molecule CT complexes. Density functional theory (DFT) calculation has revealed low-energy CT bands in the near infrared (NIR) region up to 2000 nm for graphene-TCNQ (tetracyanoquinodimethane), graphene-F_4TCNQ (2,3,5,6-Tetrafluoro-tetracyanoquinodimethane) and graphene-TCOQ (tetrachloro-o-benzoquinone) complexes. Raman and electrical measurements have confirmed a partial charge transfer between graphene and the molecules at the ground state. CT excitations have been calculated by DFT and verified by optoelectronic measurements. The graphene-organic CT complexes have shown a broadband photoresponse from visible to NIR range, attributing to the inter-molecule electronic transitions. Further, the photo-responsivity (up to 10^3 A/W) suggests a high photoelectrical gain arising from the photogating effect at the graphene/molecule interface. At last, the photoresponse property of the graphene-organic CT complexes can be tuned by electrical gating of graphene.

Since the discovery of tetrathiafulvalene-tetracyanoquinodimethane (TTF-TCNQ) charge transfer (CT) complex in 1973[1], CT complex consisting of electron donors and electron acceptors has attracted great interest due to its unique electrical[2-4], optical[3-8] and magnetic[9,10] properties. Owing to the molecular orbital overlapping and hybridization, CT complex has unique low-energy inter-molecule electronic transitions down to near infrared (NIR) region[11-14]. The inter-molecule electronic transition accomplishes high efficient charge separation and hence has great potentials in high-efficiency solar cells[15,16] and high-performance photodetectors[14].

Graphene[17], a layer of honeycomb sp^2 carbon atoms with delocalized π electron system, is a promising candidate for CT complexes with atomic thickness[18]. Due to the continuous electronic states in graphene, graphene-based CT complexes can have broadband inter-molecule CT transitions down to infrared (IR) range. Further, the charge separation at the two-dimensional interface can make graphene-based CT complexes favorable for high-gain photodetection, in which the separated charges in graphene can circulate millions of circles before recombination with the opposite charges in the molecules due to the extremely high carrier mobility in graphene[19-25] and slow charge recombination rate between graphene and the molecules.

In the past years, graphene-organic molecule interactions[26], such as doping[27-32], excited state charge/energy transfer[8,33-35], have been intensively investigated. However, inter-molecule electronic transition between graphene and organic molecules, i.e., CT transition, has not been reported. Here we have calculated electronic structure of graphene-organic CT complexes, a new kind of two-dimensional CT complex consisting of a conductive conjugated atomic layer and a layer of molecules. The investigated molecules include tetracyanoquinodimethane (TCNQ), 2,3,5,6-tetrafluoro-tetracyanoquinodimethane (F_4TCNQ) and tetrachloro-o-benzoquinone (TCOQ). Taking graphene-TCNQ CT complex as an example, density functional theory (DFT) calculation has revealed inter-molecule CT transitions covering a spectrum range from 500 to 2400 nm. Field-effect transistors (FETs) of graphene-TCNQ CT complex has been fabricated and showed ultrahigh NIR photoresponse from visible to 2000 nm with a peak responsivity higher than 2000 A/W. In addition, the photoresponse can be tuned by electrical gating of graphene.

Figure 1 shows calculated electronic structure of graphene-TCNQ CT complex. The Mulliken charge analysis shows that there is 0.18 *e* transferred from graphene to TCNQ per molecule. The optimized structure is shown in Figure 1a. The partial density of states (PDOS) is shown in Figure 1b. The Fermi level in graphene is shifted down by 0.2 eV from the Dirac point, resulting from the electron transfer from graphene to TCNQ at the ground state. Absorption spectrum is calculated for graphene-TCNQ complex, showing three new peaks at longer wavelengths (~600, 900 and 1750 nm, Figure 1c). The three

peaks correspond to electronic transitions from the highest occupied molecule orbital (HOMO) to three unoccupied orbitals. The HOMO is mainly contributed by graphene (96%) while the three unoccupied orbitals are contributed by both graphene (48% to 64%) and TCNQ (52% to 36%) (Figure 1c insets). This suggests that the three electronic transitions involve partial electron transfer from graphene to TCNQ, i.e., inter-molecule CT transitions. Similar results have been observed for graphene-F_4TCNQ and graphene-TCOQ CT complexes (Figure S1 and S2). In brief, graphene-F_4TCNQ shows CT bands around 900, 1900 nm and graphene-TCOQ shows CT bands around 900 nm.

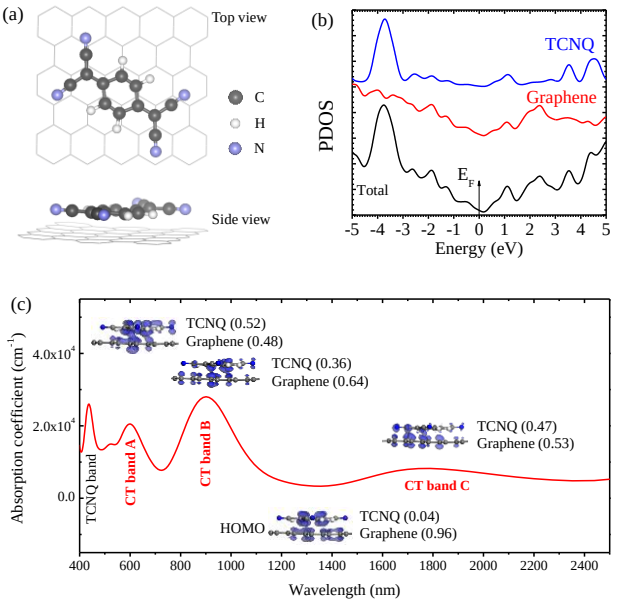

Figure 1. Calculated electronic structure of graphene-TCNQ change transfer (CT) complex. (a) CT complex structure, (b) partial density of states (PDOS) and (c) calculated absorption spectrum of graphene-TCNQ CT complex. Insets in panel c are the highest occupied molecule orbital (HOMO) and unoccupied orbitals (corresponding to the CT bands). The numbers are the orbital contributions of graphene or TCNQ.

Graphene was exfoliated on SiO_2/Si substrates and then soaked in TCNQ solution for molecule adsorption. Scanning tunneling microscopic (STM) imaging confirmed TCNQ adsorption on graphite surface (Figure 2a inset). Raman spectroscopic characterization showed an upshift of the G band from 1584 to 1589 cm^{-1} (Figure 2b), indicating a *p*-doping effect. This is consistent with the DFT calculation result of electron transfer from graphene to TCNQ at the ground state. This *p*-doping effect of TCNQ on graphene was also observed from field-effect transport measurements (Figure 2c,d), in which the minimum conductance point (the Dirac point) shifted to a more positive gate voltage after TCNQ adsorption.

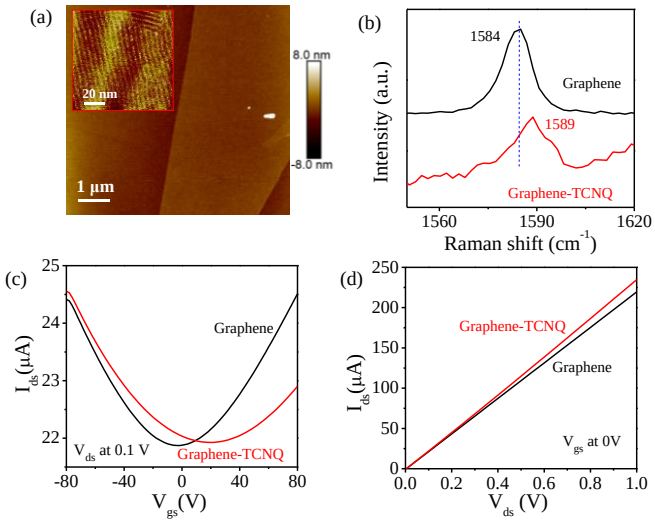

Figure 2. Characterization of graphene-TCNQ CT complex. (a) A typical atomic force microscopic (AFM) image of graphene. The inset is a scanning tunneling microscopic (STM) image of adsorbed TCNQ molecules on graphite. (b) Raman spectra, (c) Source-drain current (I_{ds}) to gate-source voltage (V_{gs}) curves and (d) I_{ds} to source-drain voltage (V_{ds}) curves of graphene before and after TCNQ adsorption.

Further, graphene-organic CT complexes were put under NIR light illumination for photoresponse measurements (Figure 3a). For the graphene-TCNQ device shown in Figure 2c, a photocurrent of μA level was observed under 1000 nm illumination with powers from 0.35 nW to 0.19 μW (Figure 3b). Since graphene was gated at *p*-type region (V_{gs} was -40 V), the positive photocurrent indicates hole injection into graphene at light illumination. That is consistent with DFT calculation result, i.e., the CT bands associate electron transfer from graphene to TCNQ (Figure 1c).

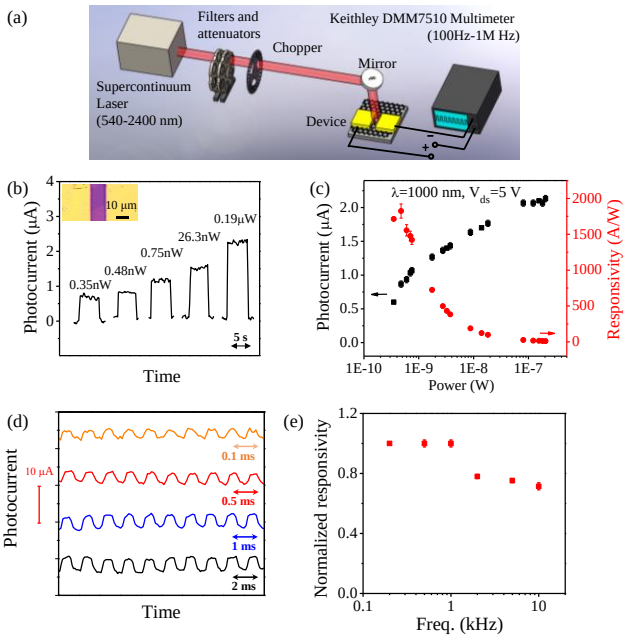

Figure 3. Photoresponse of graphene-TCNQ charge transfer (CT) complex. (a) Scheme of photocurrent measurement setup. (b) photoresponse (base current was subtracted), (c) extracted photocurrent and responsivity of graphene-TCNQ complex

measured at 1000 nm with different powers. The inset in (b) is a typical optical image of graphene-TCNQ device. (d,e) photoresponse of graphene-TCNQ complex at different chopping frequencies.

The photoresponsivity of graphene-TCNQ complex at low light illumination was as high as ~2000 A/W (Figure 3c, red data), indicating an ultrahigh photoelectrical gain. Similarly, high responsivity up to 120 A/W (at 1000 nm) and 240 A/W (at 1000 nm) were observed for graphene-F_4TCNQ and graphene-TCOQ complexes, respectively (Figure S3 and S4). The gain is attributed to the photogating effect[20,36,37], i.e., the holes in graphene circulate many times in the device before recombination with electrons in TCNQ due to the extremely high carrier mobility in graphene and slow charge recombination rate between graphene and TCNQ. As light power increased, the photocurrent increased but not linearly (Figure 3c). This is a saturation effect which is commonly observed in graphene[20,22] and MoS_2[38,39] based photogating photodetectors. The photoresponse speed was also measured by light chopping. As the light chopping frequency increased to 10 kHz, the responsivity only dropped about 30% (Figure 3d,e). This suggests that the electron-hole recombination rate in graphene-TCNQ is still faster than 0.1 ms.

Further, wavelength-dependent photoresponse of graphene-organic CT complex was measured (Figure 4). Graphene-TCNQ complex has a broad photoresponse from visible to 2000 nm. While graphene-F_4TCNQ and graphene-TCOQ have photoresponse from visible to 1200 nm. The wavelength-dependent responsivity (in A/W) matches well with the calculated absorption spectrum below 1200 nm. For graphene-TCNQ complex, at longer wavelength from 1400 to 2000 nm, the measured photoresponse is lower than the calculated absorption, in which the explanation is not clear and it needs further investigation.

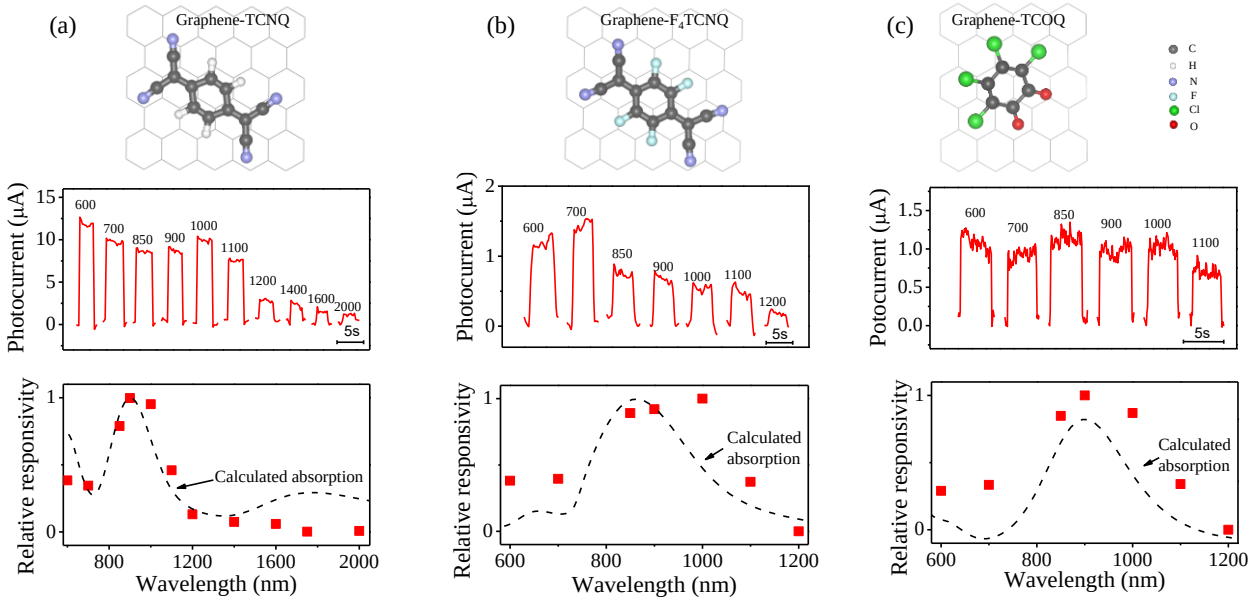

Figure 4. Wavelength-dependent photoresponse of (a) graphene-TCNQ, (b) graphene-F_4TCNQ and (c) graphene-TCOQ charge transfer (CT) complexes. The light power at different wavelengths is shown in Figure S5.

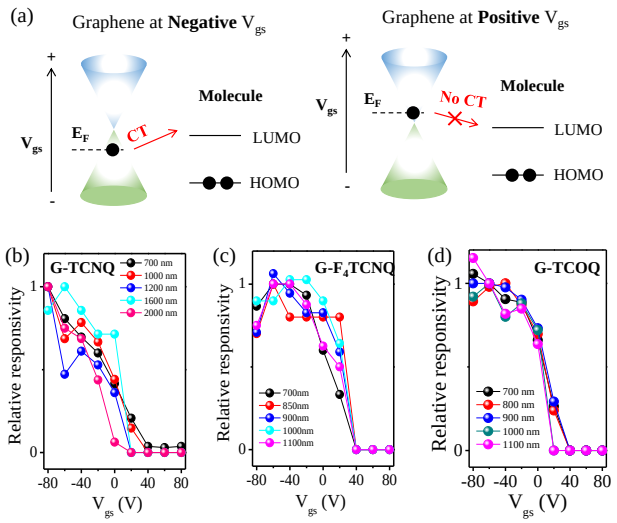

Figure 5. (a) Charge-transfer (CT) transitions in graphene-organic CT complex at different gate voltages. Gate-dependent photoresponse of (b) graphene-TCNQ, (c) graphene-F_4TCNQ and (d) graphene-TCOQ CT complexes.

The Fermi level of graphene can be tuned by the gate voltage[17,40]. At negative gate voltages, graphene is *p*-doped with major carriers of holes. In a quantitatively picture, considering graphene Dirac point at -4.6 eV and the lowest unoccupied molecule orbital (LUMO) of TCNQ, F_4TCNQ, TCOQ at -4.6[41], -5.2[42] and -4.5 (our calculation) eV, respectively, the charge (electron) transfer transition is allowed from graphene to LUMO of the molecules (Figure 5a left panel). However, when the Fermi level of graphene rises to a *n*-doped region at strong positive gate voltages, the Fermi level of graphene is higher than the LUMO of the molecules. As a result, the charge (electron) transfer transition from graphene to organic molecule is blocked (Figure 5a right panel).

In experiments, strong photoresponse was observed at negative gate voltages while no photoresponse was observed at gate

voltages higher than 40 V for all graphene-TCNQ, graphene-F_4TCNQ and graphene-TCOQ complexes (Figure 5b,c,d). This is consistent with the quantitative picture shown in Figure 5a. Therefore, the external electrical gating can be used to tune electronic excitations in graphene-organic CT complexes.

In conclusion, we have calculated the electronic structure of graphene-organic CT complexes: a new type of CT complexes with broadband NIR CT transitions. Taking advantages of the high carrier mobility of graphene and the photogating effect at graphene/molecule interface, high photoresponsivity (up to 2000 A/W) and high speed (10 kHz) photodetection have been measured from graphene-organic CT complexes. This provides a new type of tailorable NIR optical materials with potential applications in highly responsive photodetectors.

MATERIAL AND METHODS

DFT calculation. All electronic and optical properties are calculated with plane-wave pseudopotential package CASTEP. It has been confirmed by previous calculation that local density functionals could describe the electronic structure of graphene quite accurately. PBE-style GGA functional was used for all the calculation. A graphene supercell of 12 Å × 12 Å was constructed with different molecule absorbed on just one side. The van der Waals interaction was included in the empirical TS scheme. The structure was relaxed by BFGS scheme with a residual force smaller than 0.01 eV/Å. A standard ultrasoft pseuopotential was used with a cut off energy of 450 eV. Only Γ point was used for geometry optimization while a 3×3 Monkhorst-Pack grid was used for electronic and optical properties calculation.

Materials. TCNQ (PN#1427366, 98%), F_4TCNQ (PN#2157887, 97%) and TCOQ (PN#1309782, 97%) were purchased from Sigma Aldrich.

Characterization. AFM (Dimension 3100, Veeco, America) was performed with tapping mode. STM (Nanoscope IIIa, Bruker, Germany) images were conducted at I_{set} =491.3 pA, V_{bais} =559.1 mV. Raman spectrum was measured on a home-built setup with 532 nm continuous laser and the laser power was below 0.2 mW/μm^2.

Device fabrication. Graphene flakes were obtained by mechanical exfoliation of Kish graphite (Covalent Material Corp., Japan) on a silicon wafer with 300 nm SiO_2 layer. Copper TEM grid with 10 μm spacing was used as a shadow mask. 10 nm Ti and 50 nm Au were deposited for the electrodes. After evaporation, the electrodes and back silicon gate were wired to a home-made chip carrier. The device was then immersed in TCNQ, F_4TCNQ or TCOQ saturated solution in acetone for adsorption and dried in N_2 blow before photocurrent measurements.

Photoresponse measurement. The photocurrent measurement system was home-built with a pulsed laser (EXR-4, NKT, Denmark, output wavelength from 540 to 2400 nm). A series of bandpass filters from 700 nm to 2000 nm (FKB-VIS-40, FKB-IR-10, FB1750-500 and FB2000-500, Thorlabs Inc., USA) and neutral density filters (GCC-301041, GCC-301061 and GCC-301071, Daheng Optics, China; NENIR10A, NENIR20A and NENIR30A, Thorlabs Inc., USA) were used to select the output wavelength and output power. The light spot diameter was about 2 mm. The laser power under each condition was measured by a power meter (PM100A, Thorlabs Inc., USA) with different sensors suitable for the various wavelengths. The photoresponse rate was measured by an amperemeter (DMM7510, Tektronix Inc., USA) with light chopping up to 10 kHz (MC2000B, Thorlabs Inc., USA).

ASSOCIATED CONTENT

Supporting Information

Calculated electronic structure, and calculated absorption spectrum of graphene-F_4TCNQ and graphene-TCOQ change transfer (CT) complex, characterizations and photoresponse of graphene-F_4TCNQ and graphene-TCOQ, laser power at different wavelengths used in Figure 4.

AUTHOR INFORMATION

Corresponding Author

*xielm@nanoctr.cn, Tel.: +8610-82545722.
*yuzheng.guo@swansea.ac.uk, Tel.: +44-1792602994

Notes

The authors declare no competing financial interests.

ACKNOWLEDGMENT

L.X. acknowledges support from the Key Research Program of Frontier Sciences of CAS (QYZDB-SSW-SYS031), NSFC (21673058) and Beijing Talents Fund (2015000021223ZK17).

REFERENCES

(1) John, F. ; Cowan, D. O.; Walatka, V.; Perlstein, J. H. *J. Am. Chem. Soc.* **1973**, *95*, 3.
(2) Goetz, K. P.; Vermeulen, D.; Payne, M. E.; Kloc, C.; McNeil, L. E.; Jurchescu, O. D. *Journal of Materials Chemistry C* **2014**, *2*, 3065.
(3) Goetz, K. P.; Tsutsumi, J. y.; Pookpanratana, S.; Chen, J.; Corbin, N. S.; Behera, R. K.; Coropceanu, V.; Richter, C. A.; Hacker, C. A.; Hasegawa, T.; Jurchescu, O. D. *Advanced Electronic Materials* **2016**, *2*, 1600203.
(4) Abdou, M. S. A.; Orfino, F. P.; Son, Y.; Holdcroft, S. *J. Am. Chem. Soc.* **1997**, *119*, 4518.
(5) Manna, A. K.; Pati, S. K. *Chemistry – An Asian Journal* **2009**, *4*, 855.
(6) Rabie, U. M. *J. Mol. Struct.* **2013**, *1034*, 393.
(7) Lei, Y. L.; Liao, L. S.; Lee, S. T. *J. Am. Chem. Soc.* **2013**, *135*, 3744.
(8) Lei, Y.-L.; Jin, Y.; Zhou, D.-Y.; Gu, W.; Shi, X.-B.; Liao, L.-S.; Lee, S.-T. *Adv. Mater.* **2012**, *24*, 5345.
(9) Shil, S.; Paul, S.; Misra, A. *The Journal of Physical Chemistry C* **2013**, *117*, 2016.
(10) Enoki, T.; Miyazaki, A. *Chem. Rev.* **2004**, *104*, 5449.
(11) Friedrich, H. B.; Person, W. B. *The Journal of Chemical Physics* **1966**, *44*, 2161.
(12) Wu, S. P.; Kang, Y.; Liu, T. L.; Jin, Z. H.; Jiang, N.; Lu, Z. H. *Appl. Phys. Lett.* **2013**, *102*, 163304.
(13) Cameron, L. A.; Ziller, J. W.; Heyduk, A. F. *Chemical Science* **2016**, *7*, 1807.
(14) Ng, T.-W.; Lo, M.-F.; Fung, M.-K.; Zhang, W.-J.; Lee, C.-S. *Adv. Mater.* **2014**, *26*, 5569.
(15) Deibel, C.; Strobel, T.; Dyakonov, V. *Adv. Mater.* **2010**, *22*, 4097.
(16) Vandewal, K.; Gadisa, A.; Oosterbaan, W. D.; Bertho, S.; Banishoeib, F.; Van Severen, I.; Lutsen, L.; Cleij, T. J.; Vanderzande, D.; Manca, J. V. *Adv. Funct. Mater.* **2008**, *18*, 2064.

(17) Novoselov, K. S.; Geim, A. K.; Morozov, S. V.; Jiang, D.; Zhang, Y.; Dubonos, S. V.; Grigorieva, I. V.; Firsov, A. A. *Science* **2004**, *306*, 666.
(18) Muruganathan, M.; Sun, J.; Imamura, T.; Mizuta, H. *Nano Lett.* **2015**, *15*, 8176.
(19) Vicarelli, L.; Vitiello, M. S.; Coquillat, D.; Lombardo, A.; Ferrari, A. C.; Knap, W.; Polini, M.; Pellegrini, V.; Tredicucci, A. *Nature Materials* **2012**, *11*, 865.
(20) Konstantatos, G.; Badioli, M.; Gaudreau, L.; Osmond, J.; Bernechea, M.; de Arquer, F. P. G.; Gatti, F.; Koppens, F. H. L. *Nature Nanotechnology* **2012**, *7*, 363.
(21) Tan, W.-C.; Shih, W.-H.; Chen, Y. F. *Adv. Funct. Mater.* **2014**, *24*, 6818.
(22) Liu, C.-H.; Chang, Y.-C.; Norris, T. B.; Zhong, Z. *Nature Nanotechnology* **2014**, *9*, 273.
(23) Seong Jun, K.; Wooseok, S.; Sungho, K.; Min, A. K.; Sung, M.; Sun Sook, L.; Jongsun, L.; Ki-Seok, A. *Nanotechnology* **2016**, *27*, 075709.
(24) Lee, Y.; Yu, S. H.; Jeon, J.; Kim, H.; Lee, J. Y.; Kim, H.; Ahn, J.-H.; Hwang, E.; Cho, J. H. *Carbon* **2015**, *88*, 165.
(25) Fang H; Hu W. *Advanced Science*, **2017**, 4, 1700323.
(26) Das, B.; Voggu, R.; Rout, C. S.; Rao, C. N. R. *Chem. Commun.* **2008**, 5155.
(27) Sun, J. T.; Lu, Y. H.; Chen, W.; Feng, Y. P.; Wee, A. T. S. *Physical Review B* **2010**, *81*, 155403.
(28) Koch, N.; Duhm, S.; Rabe, J. P.; Vollmer, A.; Johnson, R. L. *Phys. Rev. Lett.* **2005**, *95*, 237601.
(29) Hu, T.; Gerber, I. C. *The Journal of Physical Chemistry C* **2013**, *117*, 2411.
(30) Samuels, A. J.; Carey, J. D. *ACS Nano* **2013**, *7*, 2790.
(31) Du, A.; Ng, Y. H.; Bell, N. J.; Zhu, Z.; Amal, R.; Smith, S. C. *The Journal of Physical Chemistry Letters* **2011**, *2*, 894.
(32) Zhou, X.; He, S.; Brown, K. A.; Mendez-Arroyo, J.; Boey, F.; Mirkin, C. A. *Nano Lett.* **2013**, *13*, 1616.
(33) Stein, T.; Kronik, L.; Baer, R. *J. Am. Chem. Soc.* **2009**, *131*, 2818.
(34) Xie, L.; Ling, X.; Fang, Y.; Zhang, J.; Liu, Z. *J. Am. Chem. Soc.* **2009**, *131*, 9890.
(35) Ling, X.; Xie, L.; Fang, Y.; Xu, H.; Zhang, H.; Kong, J.; Dresselhaus, M. S.; Zhang, J.; Liu, Z. *Nano Lett.* **2010**, *10*, 553.
(36) Koppens, F. H. L.; Mueller, T.; Avouris, P.; Ferrari, A. C.; Vitiello, M. S.; Polini, M. *Nature Nanotechnology* **2014**, *9*, 780.
(37) Sun, Z.; Liu, Z.; Li, J.; Tai, G.-a.; Lau, S.-P.; Yan, F. *Adv. Mater.* **2012**, *24*, 5878.
(38) Lopez-Sanchez, O.; Lembke, D.; Kayci, M.; Radenovic, A.; Kis, A. *Nature Nanotechnology* **2013**, *8*, 497.
(39) Chen, C.; Qiao, H.; Lin, S.; Man Luk, C.; Liu, Y.; Xu, Z.; Song, J.; Xue, Y.; Li, D.; Yuan, J.; Yu, W.; Pan, C.; Ping Lau, S.; Bao, Q. *Scientific Reports* **2015**, *5*, 11830.
(40) Dharmendar, R.; Leonard, F. R.; Gary, D. C.; Sanjay, K. B. J. Phys. D: Appl. Phys. 2011, 44, 313001.
(41) Kozo, M.; Jun, Y. *J. Electron. Spectrosc. Relat. Phenom*. 2009, 174, 55.
(42) Weiying, G.; Antoine, K. *Organic Electronics* **2002**, *3*, 53.

TOC

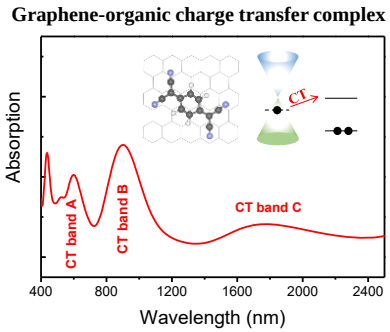
Graphene-organic charge transfer complex
Absorption
CT band A
CT band B
CT band C
CT
400
800
1200
1600
2000
2400
Wavelength (nm)